ELSEVIER

Journal of Organometallic Chemistry 572 (1999) 283–289

Journal of Organo metallic Chemistry

Synthesis, characterisation and a theoretical investigation of the formation of lithium dialkylaluminium amides

William Clegg [b], Stephen T. Liddle [b], Kenneth W. Henderson [a,*], Fiona E. Keenan [a], Alan R. Kennedy [a], Arlene E. McKeown [a], Robert E. Mulvey [a]

[a] *Department of Pure and Applied Chemistry, University of Strathclyde, Glasgow G1 1XL, UK*
[b] *Department of Chemistry, University of Newcastle, Newcastle-upon-Tyne NE1 7RU, UK*

Received 4 August 1998

Abstract

Reaction of the pre-formed crystalline amides [$(PhCH_2)_2NLi$] and [$Me_2AlN(CH_2Ph)_2$] in the presence of pyridine results in the formation of the mixed metal complex [$Me_2Al\{(PhCH_2)_2N\}_2Li \cdot pyr$] **1**. Ab initio molecular orbital calculations indicate formation of the bimetallic product is energetically favourable. Using single crystal X-ray analysis for **1** and the pyridine solvate [$\{(PhCH_2)_2NLi \cdot pyr\}_2$] **7**, in combination with theoretical calculations, the possible driving forces for the reaction are discussed. A major contributing factor in the stabilisation of the bimetallic compound was found to be a reduction in steric crowding in the mixed metal base compared to the homometallic dialkylaluminium amide. In addition, complex **1** shows significant benzyl to lithium interactions which contribute to the overall bonding. Such interactions are unusual in that donor solvent is present as competing complexant. © 1999 Elsevier Science S.A. All rights reserved.

Keywords: Lithium; Aluminium; Alkyls; Amides; Molecular orbital calculations

---

1. Introduction

Heterobimetallic combinations of Group 1 metals with other main group metallic elements represents an area of ever increasing interest [1]. Attention has mainly been directed towards mixed metal species involving lithium due to a combination of the metal's synthetic utility and ease of use [2]. A number of mixed cation organonitrogen compounds containing lithium and Group 13 metals have been structurally characterised [3–7]. To date, four synthetic methodologies have been successfully applied for the preparation of mixed lithium–aluminium organonitrogen complexes. These are (i) transmetallation of an aluminium halide with four equivalents of the lithiated organonitrogen compound [4] (ii) reaction of $LiAlH_4$ with four equivalents of amine [5] (iii) lithiation of a dialkylaluminium primary amide ($R_2AlN(H)R'$) to form the imido derivative [6] and (iv) methane elimination from an amine solvated complex of a lithium trialkylaluminium secondary amide 1–4 [7].

$$AlX_3 + 4LiNR_2 \longrightarrow 3LiX + [LiAl(NR_2)_4] \qquad (1)$$

$$LiAlH_4 + 4R_2NH \longrightarrow [LiAl(NR_2)_4] + 4H_2 \qquad (2)$$

$$[R_2AlN(H)R']_2 + 2Bu^tLi \longrightarrow [R_2AlN(Li)R']_2 + 2Bu^tH \qquad (3)$$

$$[Me_3Al(PhCH_2)_2NLi.HN(CH_2Ph)_2] \longrightarrow [Me_2Al\{(PhCH_2)_2N\}_2Li] + MeH \qquad (4)$$

In this paper an alternative synthetic strategy involving the direct reaction of pre-formed amidolithium and

---

* Corresponding author. Fax: +44-141-552-0876; e-mail: k.w.henderson@strath.ac.uk.

0022-328X/99/$ - see front matter © 1999 Elsevier Science S.A. All rights reserved.
PII: S0022-328X(98)00954-1

dialkylaluminium amide has been utilised to preparethe mixed metal compound [$Me_2Al\{(PhCH_2)_2N\}_2Li\cdot pyr$] **1**. An ab initio molecular orbital study of the homometallic precursor complexes and the mixed metal products has been used to investigate the energetics of the reaction and the driving forces for the stabilisation of the bimetallic product.

2. Results and discussion

2.1. X-ray crystallographic studies

Pure crystalline samples of lithium dibenzylamide [8] [$(PhCH_2)_2NLi$] **2** and dimethyl(dibenzylamido)-aluminium [$Me_2AlN(CH_2Ph)_2$] **3** were prepared and stored in an argon filled glove box. The solids were then mixed in a 1:1 molar ratio and suspended in toluene. One equivalent of pyridine was added to the reaction mixture and the resultant deep red solution precipitated complex **1** on cooling. An alternative synthesis involved thermolysis of the amine solvated complex [$Me_3Al\{(PhCH_2)_2N\}_2Li\cdot HN(CH_2Ph)_2$] in a pyridine/toluene mixture [7]. The identical composition of the products from these reactions was confirmed by ^{1}H-NMR spectroscopy.

An X-ray crystallographic study of **1** revealed a 1:1 complex between **2** and **3** with the lithium atom being monosolvated by a single pyridine molecule (Fig. 1, crystallographic data are given in Table 1). Bridging amido anions link the aluminium and lithium centres, resulting in a central four-membered $\mathrm{Li\overline{NAlN}}$ ring.

Several complexes containing this bridging motif have previously been characterised, including the closely related THF solvated analogue of **1** [$Me_2Al\{(PhCH_2)_2N\}_2Li\cdot THF$] **4** [7]. Another two complexes related to **1** are [$Mes_2Al(NH^tBu)_2Li\cdot THF$] [6] **5** and [$(^tBu)_2Al\{Ph_3C(H)N\}_2Li$] [9] **6**, which are both derived from primary amines (RNH_2). As expected, comparison of the core dimensions between **1** and **4** finds only very small variances. The only notable difference is the substitution of the Li(1)–N(3) dative bond (2.027(5) Å) in **1** for the Li(1)–O(1) dative bond (1.91(1) Å) in **4**, following the replacement of pyridine for THF. All other dimensions, including the orientations of the benzyl groups, are similar in both structures (a detailed examination is given in the Section 2.2). Of interest is the highly pyramidal nature of the lithium atom (sum of the angles 346.9 for **1** and 336.6° for **4**). Also, the four-membered cyclic cores of **1** and **4** are non-planar (mean deviation from the plane 0.159 in **1** and 0.142 Å in **4**; sum of the endocyclic bond angles 354.7 for **1** and 355.8° in **4**). Key bond lengths and angles for **1** are listed in Table 2.

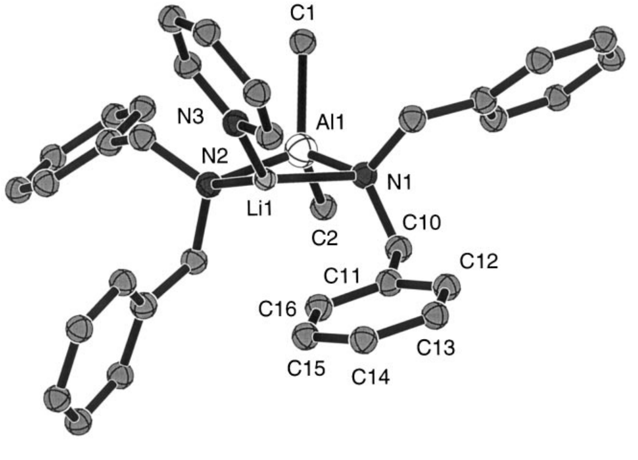

Fig. 1. Molecular structure of **1** with hydrogen atoms omitted for clarity.

Table 1
Crystallographic data

Compound	1	7
Empirical formula	$C_{35}H_{39}AlLiN_3$	$C_{38}H_{38}Li_2N_4$
M	535.61	564.60
Crystal system	Orthorhombic	Triclinic
Space group	$P2_12_12_1$	$P\bar{1}$
Unit cell dimensions		
a (Å)	15.661(4)	9.2461(17)
b (Å)	20.052(3)	9.4721(17)
c (Å)	9.840(2)	10.593(2)
α (°)	90	88.762(5)
β (°)	90	76.565(4)
γ (°)	90	67.282(5)
V (Å^3)	3090.2(11)	829.9(3)
Z	4	1
$D_{calc.}$ (g cm^{-3})	1.151	1.130
μ (mm^{-1})	0.093	0.066
F(000)	1144	300
Temperature (K)	123	160
Crystal Size (mm)	0.70 × 0.60 × 0.60	0.68 × 0.42 × 0.36
θ_{max} (°)	30.0	28.6
Maximum indices hkl	22, 28, 13	12, 12, 13
Reflections measured	5484	6120
Unique reflections	5446	3701
R_{int}	0.0379	0.0572
No. of refined parameters	363	211
wR_2 (all data)^a	0.1513	0.1678
R_1 (observed data)^a	0.0487	0.0672
Goodness-of-fit	1.050	0.877
Max/min el. density (e Å^{-3})	0.446, −0.663	0.359, −0.371

^{a} $wR_2 = \{\Sigma[w(F_o^2 - F_c^2)^2]/\Sigma[w(F_o^2)^2]\}^{1/2}$, $R_1 = \Sigma\|F_o| - |F_c\|/\Sigma|F_o|$.

The structures of the homometallic reagents are of interest when considering the possible mechanism of formation of **1**. Reaction of pre-formed crystalline **2** with one equivalent of pyridine in toluene solution yielded a red solution. Standing this solution at room temperature (r.t.) deposited crystals of the solvated complex [$\{(PhCH_2)_2NLi\cdot pyr\}_2$] **7** which was characterised by ^{1}H-NMR spectroscopy and single crystal X-ray analysis. In the solid state **7** is found to be dimeric,

Table 2
Key distances (Å) and angles (°) for **1**

Bond distance (Å)			
Al1–N1	1.904(2)	Al1–N2	1.934(2)
Al1–C1	1.980(3)	Al1–C2	1.982(3)
Al1···Li1	2.652(5)	N1–Li1	2.078(5)
N2–Li1	2.063(6)	N3–Li1	2.027(5)
Bond angle (°)			
N1–Al1–N2	98.76(9)	N1–Al1–C1	106.13(12)
N1–Al1–C2	113.03(11)	C1–Al1–C2	116.86(14)
N2–Al1–C1	111.47(11)	N2–Al1–C2	113.03(11)
Al1–N1–C3	121.14(16)	Al1–N1–C10	120.74(17)
C3–N1–C10	110.4(2)	C3–N1–Li1	108.5(2)
C10–N1–Li1	107.0(2)	Al1–N2–C17	118.14(16)
Al1–N2–C24	112.14(15)	Al1–N2–Li1	83.07(16)
C17–N2–C24	111.3(2)	C17–N2–Li1	118.8(2)
C24–N2–Li1	110.6(2)	C31–N3–C35	116.9(3)
C31–N3–Li1	120.4(3)	C35–N3–Li1	122.1(2)
N1–C3–C4	116.8(2)	N1–C10–C11	111.53(19)
N2–C17–C18	114.4(2)	N2–C24–C25	117.3(2)
Al1–Li1–N3	139.8(2)	N1–Li1–N2	89.4(2)
N2–Li1–N3	128.3(3)	N1–Li1–N3	129.2(3)

bridging through the amido anions and with each lithium terminally solvated by one pyridine molecule (Fig. 2).

The structural chemistry of the lithium dibenzylamide system has been extensively studied over the past two decades as a model for bulky amido anions [10]. As found in **7** the most common structural motif for solvates of lithium dibenzylamide is that of a disolvated dimeric ring. A closely related analogue of **7** is the THF solvate $[\{(PhCH_2)_2NLi \cdot THF\}_2]$ **8** ([10]b). Comparison of the bond lengths and angles between **7** and **8** show only small variances. As expected, the major difference is the replacement of pyridine (Li(1)–N(2) 2.012(4) Å) for THF (Li(1)–O(1) 1.915(3) Å). The effect of solvent substitution is also seen in a shortening of the Li–N bonds of the central four-membered ring of **7** compared to **8**, Li(1)–N(1) 1.983(4) and Li(1)–N(1a) 1.988(4) Å in **7**, but Li(1)–N(1) 2.028(3) and Li(1)–N(1a) 2.058(3) Å in **8**. Nevertheless, overall the structures adopt very similar gross geometrical features. Key bond lengths and angles for **7** are given in Table 3.

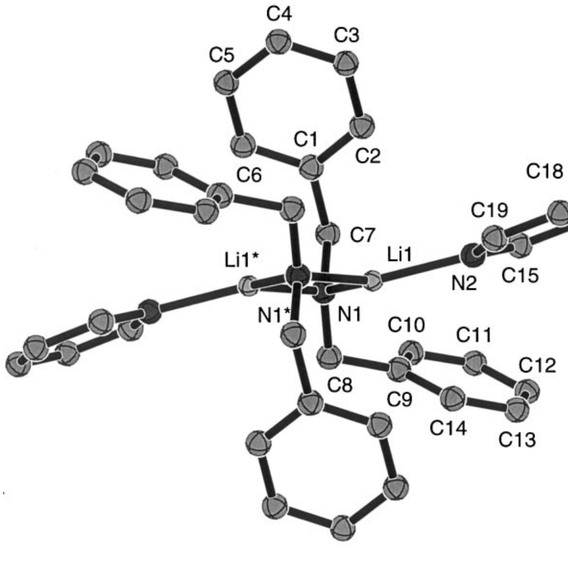

Fig. 2. Molecular structure of **7** with hydrogen atoms omitted for clarity.

Table 3
Key distances (Å) and angles (°) for **7**

Bond distance (Å)			
Li1–N1	1.983(4)	Li1–N1a	1.988(4)
Li1–N2	2.012(4)	Li1···Li1a	2.410(7)
Bond angle (°)			
N1–Li1–N1a	105.29(16)	N1–Li1–N2	129.53(19)
N1a–Li1–N2	123.43(18)	C7–N1–Li1	116.59(18)
C7–N1–Li1a	116.43(16)	C7–N1–C8	110.25(15)
C8–N1–Li1	119.00(16)	C8–N1–Li1a	116.06(17)
Li1–N1–Li1a	74.71(16)	N1–C8–C9	114.45(17)
N1–C7–C1	110.47(15)		

2.2. Theoretical calculations

Ab initio molecular orbital calculations run at the HF/6-31G* level were used to probe the nature of the reaction between the homometallic bases. Initially dimethylamido units were used to model the dibenzylamido anions to simplify the calculations. Dimers were taken to be the most likely structures for the homometallic bases. This is the most common structural arrangement for dialkylaluminium amides [11] and solvated amidolithiums. The homometallic starting materials $[\{Me_2AlNMe_2\}_2]$ **I** and $[\{Me_2NLi \cdot pyr\}_2]$ **II** and the heterobimetallic complex $[Me_2Al(Me_2N)_2Li \cdot pyr]$ **III** were geometry optimised with no imposed constraints. Figs. 3–5 show the energy minima geometries with selected bond lengths, bond angles and charges. A comparison of the geometry of **I** with its known crystal structure shows excellent agreement, with the average difference between the bond lengths and between the angles being (<0.05 Å) and ($<1°$), respectively ([11]a).

Table 4 lists the energies of the calculated structures. The energy of the reaction between **I** and **II** to form two equivalents of **III** is calculated to be exothermic by -18.40 kcal mol^{-1}. An inspection of the bond lengths and angles within the structures of **I**–**III** gives some indication of the source of this stabilisation. The core ring in **II** is distinctly rhomboidal with large N–Li–N angles of 106.8° and acute Li–N–Li angles of 73.2°. In contrast the core of **I** is much nearer to a square with N–Al–N angles of 88.1 and Al–N–Al angles of 90.9°. Ring angles in **III** are intermediate between these two extremes with N–Li–N at 93.2, N–Al–N at 96.9 and Li–N–Al at 83.6°. The dimeric rings in **I** and **III** are

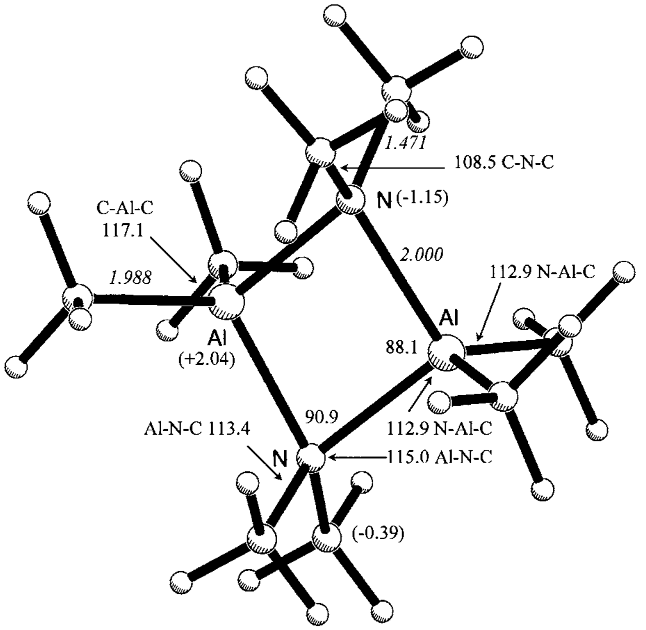

Fig. 3. Energy minimum calculated structure of **I**, showing bond angles (°) as normal text, bond lengths (Å) in italics and atomic charges in brackets.

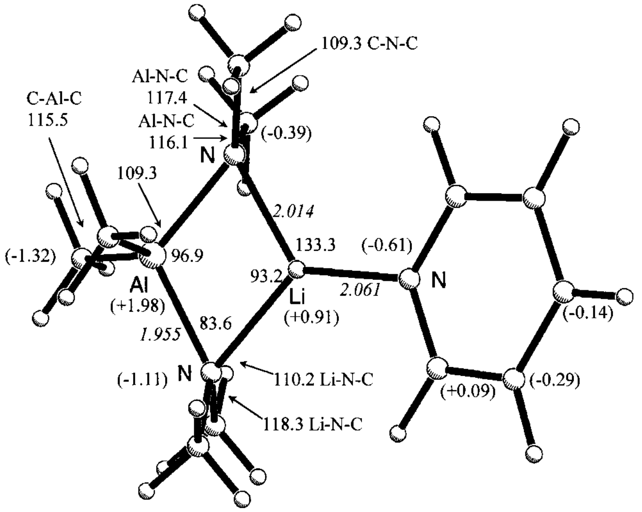

Fig. 5. Energy minimum calculated structure of **III**, showing bond angles (°) as normal text, bond lengths (Å) in italics and atomic charges in brackets.

puckered with the sum of the endocyclic bond angles being 358.0 for **I** and 357.6° for **III**. Puckering of the ring aids in relieving torsional strain induced by adjacent methyl groups. If all the methyl groups in **I** are replaced by hydrogens to give [$\{H_2AlNH_2\}_2$] **IV**, the ring reverts to planarity. Adding methyl groups to the aluminium, i.e. [$\{Me_2AlNH_2\}_2$] **V**, or the amido nitrogen in isolation, i.e. [$\{H_2AlNMe_2\}_2$] **VI**, also has no effect on the planarity of the ring. Placing methyl groups on both the aluminiums and the amido nitrogens induces puckering. This is reflected in the torsional angles R–Al–N–R (for syn substituents) lying between 5.1 and 7.8° for the planar rings in **IV**–**VI**, whereas substantially more staggered angles are found in **I** and **III**, 16.9, 8.7, 18.0 and 20.5°, respectively. Hence, the cause of this distortion is the reduction of repulsions between adjacent methyl groups on the periphery of the dimeric ring. Another important effect on moving from **I** to **III** is the change in the N···N distance (N···N 2.78 in **I**, 3.20 in **II** and 2.92 Å in **III**) which occurs with a concomitant change in metal–metal separations (Al···Al 2.84 in **I**, Li···Li 2.38 in **II** and Li···Al 2.65 Å in **III**). These effects combine to make formation of the bimetallic compound thermodynamically favourable.

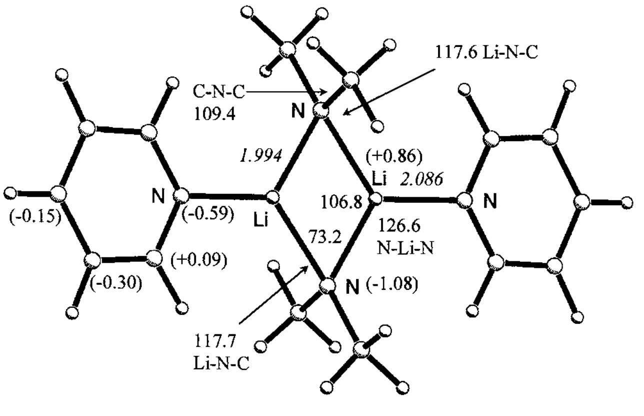

Fig. 4. Energy minimum calculated structure of **II**, showing bond angles (°) as normal text, bond lengths (Å) in italics and atomic charges in brackets.

A comparison of theoretical and experimental bond lengths and angles shows good agreement. One noticeable difference between the calculated model **III** and the experimental structure of **1** is the positioning of the pyridine solvent molecule. In **III** the Al(1)–Li(1)–N(3) angle is 173.0° whereas a much more acute angle of 139.8° is found in **1**. This is due to the pyridine molecule in the crystal **1** sitting out the 'plane' of the buckled $\overline{\text{LiNAlN}}$ ring. To investigate if this is a consequence of steric influences a calculation was run on a more realistic model, where the methyl groups on the amide were replaced by benzyl units to give the actual

Table 4
Calculated energies (Hartrees) of the complexes

Compound	Total energy (Hartrees)
I	−909.747528082
II	−775.726802458
III	−842.751823916
IV	−597.490159408
V	−753.668756250
VI	−753.574249292
VII	−1760.93313543
VIII	−1693.92484358

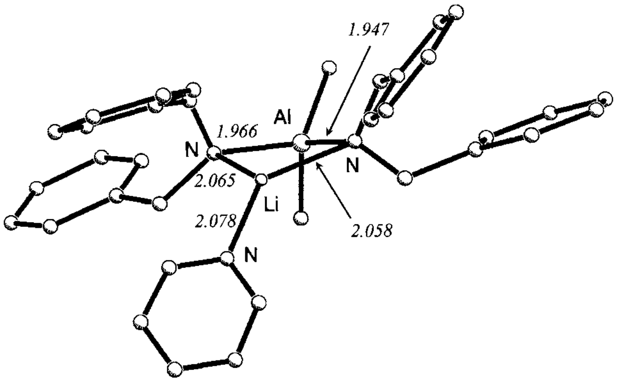

Fig. 6. Energy minimum calculated structure of **VII**, showing bond lengths (Å) in italics.

composition of **1** i.e. $[\mathrm{Me_2Al\{N(CH_2Ph)_2\}Li\cdot pyr}]$ **VII** (Fig. 6).

The model complex **VII** optimised to a structure very similar in geometry to that of **1**. Indeed the Al–Li–N(pyr) angle of 140.5° is remarkably close to the experimental value of 139.8°. In the THF derivative **8**, an even more acute Al–Li–O(THF) angle of 130.8° was found. In this case the larger size of THF compared to the flat pyridine forces the solvent even further out of the dimeric plane. In contrast, the homometallic lithium amide complex **II** has planar solvation of the dimeric ring by pyridine (Li–Li–N(pyr) 180.0°). As before, to investigate if increasing the steric bulk on nitrogen affects the solvation mode, a calculation was run by replacing the methyl groups for benzyl units to give a complex with the same composition as **7** i.e. $[\{\mathrm{(PhCH_2)_2NLi\cdot pyr}\}_2]$ **VIII** (Fig. 7).

The calculated structure **VIII** was found to have an Li–Li–N(pyr) angle of 170.9° which compares favourably with the experimental value of 168.1° found for **7**. Therefore changing methyl for benzyl only has a relatively small effect on the solvation mode and certainly it is a very minor change in comparison to the distinct pyramidalisation of the lithium in the heterobimetallic systems.

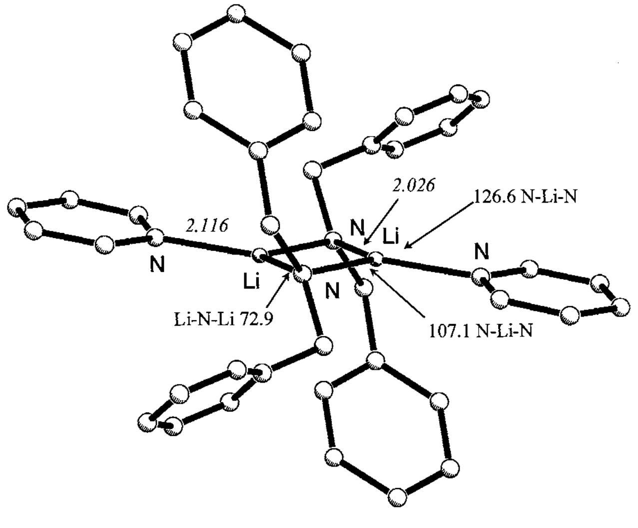

Fig. 7. Energy minimum calculated structure of **VIII**, showing bond angles (°) as normal text and bond lengths (Å) in italics.

A close examination of the crystal structure of **1** and the model structure of **VII** gives some insight into this pyramidalisation at lithium. One of the benzyl units is significantly twisted towards the lithium centre leading to relatively short Li···C(H) interactions. In **1** these contact distances are Li(1)···C(10)benzyl 2.89, Li(1)···C(11)*ipso* 2.93 and Li(1)···C(16)*ortho* 2.63 Å. Similarly, from the calculated structure of **VII** the contact distances are Li···C(benzyl) 2.88, Li···C(*ipso*) 3.05 and Li···C(*ortho*) 3.02 Å. The significance of these benzyl to lithium interactions is highlighted when compared to the previously calculated structure of unsolvated monomeric lithium dibenzylamide $[\mathrm{(PhCH_2)_2NLi}]$ **IX** [12]. The geometry optimised structure of **IX** has both phenyl rings directed towards the lithium. The shortest Li–C contacts are Li···C(benzyl) 2.85, Li···C(*ipso*) 2.90 and Li···C(*ortho*) 3.36 Å. These interactions, although not particularly short, account for a stabilisation of -14.3 kcal mol^{-1} compared with the geometry where the phenyl rings are directed away from lithium. Hence, since the Li···C(H) contact distances calculated for **VII** are similar to those of **IX**, they may make a contribution to the stability of the heterodimer.

That this interaction occurs in the heterodimer and not the homodimer is probably due to substituting a trigonal planar lithium by a pseudo-tetrahedral aluminium. The projection of the methyl groups on aluminium above and below the plane of the dimeric ring causes the proximate benzyl groups to move towards the lithium. This is seen in the distortion of the angles around one of the amido nitrogens (N(1)), where there is significant tilting towards lithium (Li(1)–N(1)–C(benzyl) mean angle in **1** is 107.8° and the Al(1)–N(1)–C(benzyl) mean angle is 120.9°, compared with a Li–N–C(benzyl) mean angle of 117.0° in **7**). The remaining amido anion (N(2)) has a much smaller distortion, with a mean Li(1)–N(2)–C(benzyl) at 114.6 and Al(1)–N(2)–C(benzyl) at 115.1°. As expected it is the amido anion with the greater distortion which is involved in the Li(1)···C(16) interaction. This distortion facilitates the movement of the phenyl ring towards the lithium.

Such benzyl to lithium interactions have previously been noted in several structures, including unsolvated lithium dibenzylamide which is a ring trimer [8]. Short phenyl to lithium interactions were also found in the bimetallic complex $[(^t\mathrm{Bu})_2\mathrm{Al}\{\mathrm{Ph_3C(H)N}\}_2\mathrm{Li}]$ [9]. Noteworthy is the fact that the phenyl to lithium interactions in **1** persist even though donor solvent, in the form of pyridine, is present. Generally, short contacts of this type are thought to be relatively weak, and occur only when the metal is forced into a low coordination environment. It is therefore commonplace for these interactions to disappear when Lewis base is present as complexant [13].

Another possible stabilising factor of the heterodimers is the relocation of electron density within the molecule i.e. a 'push–pull' stabilisation [14]. This was investigated by natural charge population analysis of the homometallic and heterometallic complexes **I**–**III**. Figs. 3–5 show the charges located on each atom. On changing from the homodimers **I** and **II** to bimetallic **III** there is a modest movement of electron density away from lithium towards aluminium (difference in charge is -0.06 for Al and $+0.05$ for Li). Apart from the amido nitrogen atoms, which equilibrate to a value of -1.11, the charges on the remaining atoms do not alter to any significant degree. From these calculations it appears that charge relocation makes only a minor contribution in these systems. Charges on the calculated structure of **VII** are consistent with the lithium to phenyl interaction at the *ortho* position. The charge at the *ortho* carbon in contact with lithium is -0.28 which is larger than that found for the average value of -0.23 at the remaining *ortho* positions of **VII** (Mulliken charges quoted).

In conclusion, we have shown that heterobimetallic combinations of dialkylaluminium amides and lithium amides can be prepared by simply mixing the preformed homometallic compounds in the presence of a donor solvent. Ab initio calculations indicate that the formation of the mixed metal species is energetically favourable. A major factor contributing to this energy gain is the alleviation of steric strain imposed in the dialkylaluminium amide dimer starting material. Changing from a system with four interconnected tetracoordinate atoms (i.e. two aluminiums and two nitrogens) to one in which there is one tricoordinate and three tetracoordinate atoms allows an increased degree of steric freedom. In addition, the bimetallic complex **1** gains significant stability from the formation of benzyl to lithium interactions which exist in spite of the presence of donating solvent.

3. Experimental

3.1. Syntheses

All solvents were distilled over sodium/benzophenone until blue and stored over 4A molecular sieve before use. Amines were distilled over CaH_2 prior to use. Standard Schlenk techniques [15] were employed for the preparation and manipulation of the highly air and moisture sensitive materials. All reactions were carried out under a prepurified argon blanket. Bu^nLi was standardised by titration with diphenylacetic acid before use [16]. Trimethylaluminium was purchased from Aldrich as a 1 M solution in hexane and used as received. Lithium dibenzylamide was prepared by literature methods [8]. ^{1}H-NMR spectra were recorded on a Bruker AMX 400 spectrometer at r.t.

3.1.1. Synthesis of $[Me_2AlN(CH_2Ph)_2]$

A 10 ml solution of 1 M trimethylaluminium (10 mmol) in hexanes was placed in a Schlenk tube and cooled to 0°C. Dibenzylamine (10 mmol) was added dropwise over a period of 10 min to the clear colourless solution. The solution was allowed to warm to r.t. and was then refluxed for 3 h. After cooling to r.t., the solution was stored at -28°C for 2 days. Small crystals of $[Me_2AlN(CH_2Ph)_2]$ were precipitated from solution and isolated into an argon-filled glove box. Non-optimised yield 56%. Melting point 128–130°C. ^{1}H-NMR (400 MHz, benzene-d_6): δ 0.07 (s, 6H, Al*Me*$_2$), δ 4.16 (s, 4H, PhC*H*$_2$), δ 7.03 (m, 10H, *o*, *m*, *p-Ph*)

3.1.2. Synthesis of $[Me_2Al(PhCH_2)_2NLi\cdot pyr]$ **1**

Equimolar amounts (3 mmol) of lithium dibenzylamide and $[Me_2AlN(CH_2Ph)_2]$ were added to a Schlenk tube inside an argon-filled glove box. The Schlenk tube was removed from the glove box and 10 ml of toluene added to suspend the solids. Pyridine (3 mmol) was added dropwise by syringe resulting in the dissolution of the solids and the production of a deep red solution. The solution was stirred for 2 h at r.t. and then placed in a -28°C freezer. After 24 h a pale yellow solid was precipitated from solution and isolated by filtration. Non-optimised yield 39%. Melting point 119–121°C. ^{1}H-NMR (400 MHz, benzene-d_6): δ 0.10 (s, 6H, Al*Me*$_2$), δ 4.23 (s, 4H, PhC*H*$_2$), δ 6.49 (t, 2H, *β-pyr*), δ 6.85 (t, 1H, *γ-pyr*), δ 7.06 (t, 2H, *p-Ph*), δ 7.16 (t, 4H, *o-Ph*), δ 7.23 (d, 4H, *o-Ph*), δ 7.59 (d, 2H, *α-pyr*).

3.1.3. Synthesis of $[\{(PhCH_2)_2NLi\cdot pyr\}_2]$ **7**

A Schlenk tube was charged with dibenzylamine (10 mmol) and 10 ml of toluene. Bu^nLi (10 mmol as a 1.6 M solution in hexanes) was added dropwise to the 0°C cooled solution. The solution was allowed to warm to r.t. and stirred for 1 h. Pyridine (10 mmol) was added to the solution resulting in the formation of a deep red colour. Upon standing the solution at r.t. for 24 h, crystals of **7** were deposited. Non-optimised yield 82%. Melting point 170–172°C. ^{1}H-NMR (400 MHz, d_6-DMSO): δ 3.66 (s, 4H, PhC*H*$_2$), δ 7.22 (t, 2H, *β-pyr*), δ 7.37 (m, 10H, *o*, *m*, *p-Ph*), δ 7.78 (t, 1H, *γ-pyr*), δ 8.58 (d, 2H, *α-pyr*).

3.2. X-ray crystallography

Crystallographic data is presented in Table 1. Data for **1** were collected on a Rigaku AFC7S diffractometer fitted with a graphite monochromator ($\lambda = 0.71069$ Å). Data for **7** were collected on a Bruker AXS CCD diffractometer with graphite-monochromated Mo–K_α radiation ($\lambda = 0.71073$ Å). Absorption corrections were unnecessary for both structures.

The structures were solved by automatic direct methods and refined on F^2 values for all unique data, with anisotropic displacement parameters and with a riding model for isotropic H atoms. Programs were standard diffractometer control software, members of the SHELX family (G.M. Sheldrick, University of Göttingen, Germany), and local programs.

Complete crystallographic results have been deposited at the Cambridge Crystallographic Data Centre.

3.3. Theoretical calculations

The Gaussian 94 program, revision E.2, was used for the calculations [17]. For the larger molecules **VII** and **VIII** geometry optimisation was carried out using the HF/6-31G basis set as an initial guess and then reoptimised at the higher 6-31G* level. No constraints were used in any of the optimisations.

Acknowledgements

We would like to thank the Royal Society for granting K.W. Henderson a University Research Fellowship and the EPSRC for an equipment research grant (W. Clegg). We also wish to thank BP Chemicals for partial funding (A.E. McKeown).

References

[1] (a) M.A. Beswick, D.S. Wright in: E.W. Abel, F.G.A. Stone, G. Wilkinson (Eds.), Comprehensive Organometallic Chemistry, vol. 1, 1995, ch. 1. (b) M.A. Beswick, N. Choi, C.N. Harmer, et al., Inorg. Chem. 37 (1998) 2177. (c) R.E. Mulvey, Chem. Soc. Rev. 27 (1998) 339.

[2] For uses of lithium reagents see: B.J. Wakefield, Organolithium Methods, Academic Press, London, 1988.

[3] For lithium/gallium complexes see: (a) D.A. Atwood, A.H. Cowley, R.A. Jones, Organometallics 12 (1993) 236. (b) G. Linti, H. Nöth, K. Polborn, C. Robl, M. Schmidt, Chem. Ber. 128 (1995) 487. (c) M. Niemeyer, P.P. Power, Organometallics 14 (1995) 5488. (d) S.T. Barry, D.S. Richeson, Chem. Mater. 6 (1994) 2220. For an example of a lithium/indium complex see: (e) M. Veith, M. Zimmer, S. Muller-Becker, Angew. Chem. Int. Ed. Engl. 32 (1993) 1731.

[4] H.M.M. Shearer, R. Snaith, K. Wade, J. Chem. Soc. Chem. Commun. (1971) 1275.

[5] (a) St. Böck, H. Nöth, P. Rahm, Z. Naturforsch. Teil B 43 (1988) 53. (b) M.M. Andrianarison, M.C. Ellerby, I.B. Gorrell, P.B. Hitchcock, J.D. Smith, D.R. Stanley, J. Chem. Soc. Dalton Trans. (1996) 211. (c) A. Heine, D. Stalke, Angew. Chem. Int. Ed. Engl. 31 (1992) 854. (d) M.L. Montero, H. Wessel, H.W. Roesky, M. Teichert, I. Usón, Angew. Chem. Int. Ed. Engl. 36 (1997) 629.

[6] D. Rutherford, D.A. Atwood, J. Am. Chem. Soc. 118 (1996) 11535.

[7] D.A. Armstrong, F.J. Craig, A.R. Kennedy, R.E. Mulvey, J. Organomet. Chem. 550 (1998) 355.

[8] D. Barr, W. Clegg, R.E. Mulvey, R. Snaith, J. Chem. Soc. Chem. Commun. (1984) 285.

[9] M.A. Petrie, K. Ruhlandt-Senge, P.P. Power, Inorg. Chem. 32 (1993) 1135.

[10] (a) D.R. Baker, R.E. Mulvey, W. Clegg, P.A. O'Neil, J. Am. Chem. Soc. 115 (1993) 6472. (b) P.C. Andrews, D.R. Armstrong, D.R. Baker, et al., Organometallics 14 (1995) 427. (c) D. Barr, W. Clegg, R.E. Mulvey, R. Snaith, J. Chem. Soc. Chem. Commun. (1984) 285. (d) D.R. Armstrong, R.E. Mulvey, G.T. Walker, et al., J. Chem. Soc. Dalton Trans. (1988) 617. (e) D.R. Armstrong, M.G. Davidson, D. Moncrieff, Angew. Chem. Int. Ed. Engl. 34 (1995) 478.

[11] For a review see: J.J. Eisch in: G. Wilkinson, F.G.A. Stone, E.W. Abel (Eds.), Comprehensive Organometallic Chemistry, vol. 1, Pergamon Press, Oxford, 1982, ch. 6. For some examples see: (a) H. Hess, A. Hinderer, S. Steinhauser, Z. Anorg. Allg. Chem. 377 (1970) 1. (b) T. Belgardt, J. Storre, A. Klemp, et al., J. Chem. Soc. Dalton Trans. (1995) 3747. (c) T.Y. Her, C.C. Chang, J.O. Tsai, et al., Polyhedron 12 (1993) 731.

[12] D.R. Armstrong, D.B. Baker, F.J. Craig, R.E. Mulvey, W. Clegg, L. Horsburgh, Polyhedron 15 (1996) 3533.

[13] W. Clegg, K.W. Henderson, R.E. Mulvey, P.A. O'Neil, J. Chem. Soc. Chem. Commun. (1994) 769.

[14] K.W. Henderson, A.E. Dorigo, Q-Y. Liu, P.G. Williard, P.v.R. Schleyer, P.R. Bernstein, J. Am. Chem. Soc. 118 (1996) 1339.

[15] D.F. Shriver, M.A. Drezdzon, The Manipulation of Air-Sentitive Compounds, Wiley, New York, 1986.

[16] W.G. Kofron, L.M. Baclawski, J. Org. Chem. 4 (1976) 1879.

[17] M.J. Frisch, G.W. Trucks, H.B. Schlegel, et al., Gaussian Inc., Pittsburgh PA, 1995.